Original Article | Journal of Biosystems Engineering

J. of Biosystems Eng. 38(4):327-334. (2013. 12)
http://dx.doi.org/10.5307/JBE.2013.38.4.327

eISSN : 2234-1862
pISSN : 1738-1266

Analysis and Modelling of Vibration Performance for Multi-layered Corrugated Structure

Jin Nyul Kim[1], Jae Min Sim[1], Min Jung Park[1], Ghi Seok Kim[2], Jongsoon Kim[1], Jong Min Park[1]*

[1]*Department of Bioindustrial Machinery Engineering, Pusan National University, Korea*
[2]*Division of Instrument Development, Korea Basic Science Institute, Korea*

Received: November 4th, 2013; Revised: November 19th, 2013; Accepted: November 26th, 2013

Abstract

Purpose: The purpose of this study was to analyze for resonant frequency, vibration transmissibility and damping ratio of multi-layered corrugated structures using a random vibration test. **Methods:** The random vibration test was performed by the ASTM D4728 specifications using two paperboards (S120, K180) and two types of flutes (A/F, B/F). Damping ratio of the multi-layered corrugated structures was estimated using a theoretical equation derived from the measured resonant frequency and transmissibility. **Results:** The resonant frequency and vibration transmissibility of the multi-layered corrugated structures of K180 and B-flute were higher than those of S120 and A-flute, respectively; however, the damping ratio of each sample had the opposite tendency. The resonant frequency was inversely proportional to the sample thickness and static stress; vibration transmissibility and damping ratio were not correlated with sample thickness and static stress. In addition, we developed a mathematical model of the resonant frequency with variables of sample thickness and static stress. **Conclusions:** Results of this study can be useful for environment-friendly and optimal packaging design since vibration has been a key factor in cushioning packaging design.

Keywords: Cushioning packaging design, Multi-layered corrugated structure, Random vibration test, Resonant frequency, Vibration transmissibility

Introduction

Transport packaging has been used to ensure that the products are well protected from the potentially harmful environment such as shock and vibration during distribution.

Since the working mechanism of shock for cushioning is different from the one of vibration, those two factors should be considered compromisingly in cushioning packaging design. Conventional cushioning packages were designed considering shock cushioning characteristics, and subsequently it was evaluated with the resonant response test. However, the products have been hardly damaged by shocks due to modernized logistics facilities and developed handling technique. As a result, vibration cushioning during distribution is getting more noticed in cushioning packaging design for home appliances.

In Korea, both multi-layered corrugated structure (*MLCS*) and pulp mold are used as environment-friendly cushioning materials. *MLCS* is used for both heavy-weight and light weight products because of its excellent cushioning capacity and high resistance against compression, while pulp mold is used only for light-weight products. Moreover, the process for manufacturing *MLCS* is relatively simple; thus, product's packaging development period is short. Recyclability, low cost per its volume, easy formability with standardized production facilities, and batch production are also advantages of the *MLCS*.

A *MLCS* is made by overlapping several layers of single-faced corrugated fiberboard. Angle, channel, and flat are basic form of *MLCS*, and these components could be modified for various purpose.

***Corresponding author:** Jong Min Park
Tel: +82-55-350-5424; **Fax:** +82-55-350-5429
E-mail: parkjssy@pusan.ac.kr

Various researches for the single-wall (*SW*) and double-wall (*DW*) corrugated fiberboard have been performed domestically and internationally (Guo and Zhang, 2008; Park et al., 2011; Sek and Kirkpatrick, 1997). As the public became more aware of environmental problems. a *MLCS* has been noticed as a substitute of polymer-based cushioning material; a *MLCS* was made of paper, which is biodegradable and can be easily recycled after use.

Rouillard and Sek (2007) investigated the behaviour of *MLCS* under impact loading. Guo et al. (2010) evaluate the dynamic shock cushioning property of *MLCS* by drop shock tests, and established the experimental formulas of dynamic cushioning curves. Also, they studied the vibration transmissibility of *MLCS* at different static loads, and analyzed the resonance frequencies, vibration transmissibility and damping ratios. Recently, Guo et al. (2011) evaluated the dynamic shock cushioning characteristics and vibration transmissibility of *X-PLY* corrugated paperboards by the drop shock tester and vibration tester, and the peak frequencies and vibration transmissibility measured from the experiment were used to calculate the damping ratios.

Honeycomb paperboard, which is a sandwich structure formed by two liners and one paper honeycomb core, is another type of environment-friendly packaging material. The dynamic cushion curves of honeycomb paperboard with different thickness was developed using a drop shock test (Guo and Zhang, 2004). In addition, the relative density of paper honeycomb core and the height of honeycomb paperboard have a significant effect on its cushioning properties (Wang and Wang, 2008).

Up to now, most of the researches about *MLCS* have been focused on its characteristics in a specific condition. No literature is available on modeling of vibration transmissibility which is essential for cushioning design.

Thus, the objective of this study was to analyze vibration properties such as resonant frequency, vibration transmissibility, and damping ratios of *MLCS* at different flutes and paperboards using random vibration test, and to develop model for resonance frequency.

Materials and Methods

Experimental apparatus design

As shown in Figure 1, experimental equipment for vibration transmissibility of *MLCS* was comprised of

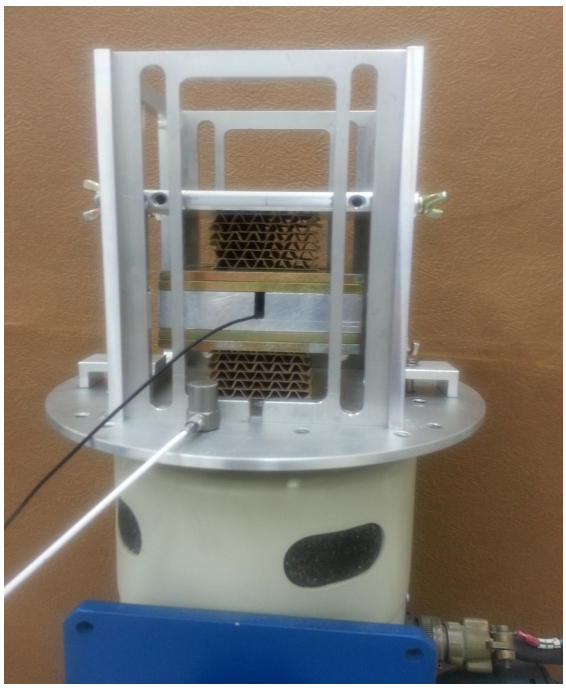

Figure 1. Experimental apparatus for vibration transmissibility.

electromagnetic shaker (LS-100, LING Electronics Inc. USA), 4-channel A/D board embedded controller to control the vibration profile, PZT accelerometer for vibration control (Kistler, range_100 G, sensitivity_50.44 mV/G, frequency response_1~25 kHz), light-weight PZT accelerometer with flexible cable for vibration signal measurement (Kistler, range_500 G, sensitivity_9.80 mV/G, frequency response_1~25 kHz) and sample fixture for fixing the sample of *MLCS* on shaker table.

The sample fixture was designed to apply the vibration force to the *MLCS* samples, and it was made of aluminum due to its rigidity and light-weight feature. The test block [(3) in Figure 2] plays a role in increasing weight on the samples. In order to accurately analyze the vibration transmissibility feature of *MLCS*, the resonant frequency on the sample fixture including the test block should not be detected in the measurement range. Figure 3 shows the preliminary test results of vibration response for sample fixture; no resonance was observed within the test frequency range. However, it has limitation in vibration control capacity in lower frequency (below 3 Hz).

Materials

Table 1 shows the flute type and paperboards specifications of *MLCS* used in the study. All these flutes and paperboard are commonly used in corrugated packages.

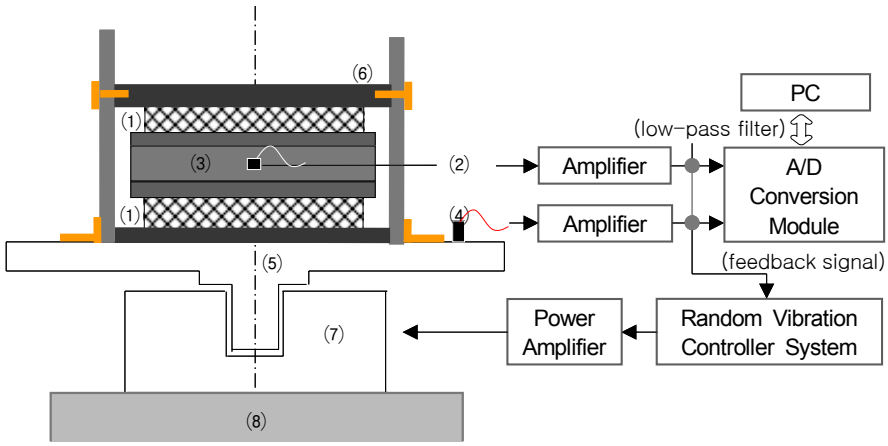

(1) test specimen, (2) response accel., (3) test block, (4) input(control) accel. (5) vibration table, (6) fixture device, (7) electro-dynamic shaker (8) seismic base

Figure 2. Schematic and block diagram of the vibration transmissibility test apparatus.

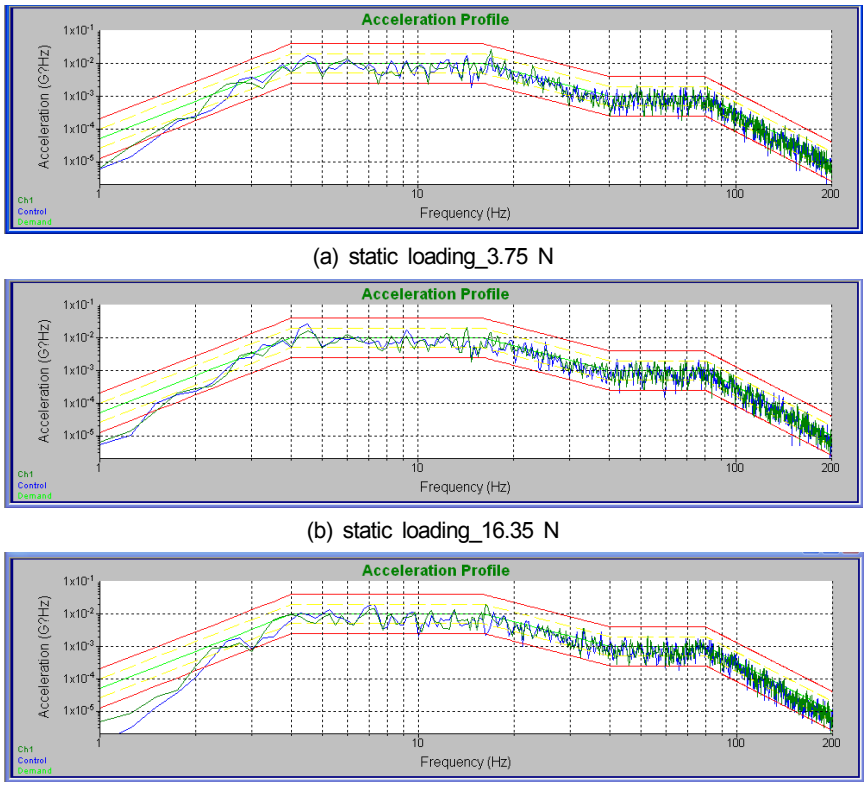

(a) static loading_3.75 N

(b) static loading_16.35 N

(c) static loading_28.75 N

Figure 3. Vibration response of sample fixture device for the range of test frequency at varying static loading.

Table 1. *MLCS* used in the vibration test

Flute type	Paperboards[a)]	Specifications
A/F	*S120*	·height, wave length, and take-up-factor of flute: *A/F*_4.6 mm, 8.8 mm, 1.6; *B/F*_2.6 mm, 6.0 mm, 1.4 ·thickness of paperboard: *K180*_0.24 mm; *S120*_0.19 mm ·ring crush: *K180*_198 N; *S120*_82 N
	K180	
B/F	*S120*	
	K180	

a) *S120* and *K180*; *KOCC* (100%), *KOCC*=korean old corrugated container

The shape of test specimen was rectangle (50×50 mm), and the experiments were conducted with three different thickness (10, 30, and 50 mm), where the corresponding static stresses (static loading/area of specimen) were 1.5, 6.5, and 11.5 kPa. The samples were preconditioned for 72 hrs at 23±2℃ and 50±2% relative humidity, and subsequently the tests were performed in the same environmental condition.

Experimental methods

A random vibration test method was used to analyze the vibration transmissibility of *MLCS*. The *PSD* (Power Spectral Density) expresses random vibration in terms of mean-square acceleration per unit of frequency (g^2/Hz) (ASTM, 2012). The *PSD* test profile for truck taken in Practice D4728 Assurance Level II (Table 2) was applied to the random vibration test. The specimens were fastened with two horizontal screws and pre-loaded with 14.72 N.

Results and Discussion

Vibration transmissibility and modelling

The non-dimensional transmissibility is defined by the ratio of its response amplitude to the excitation amplitude. In general, the shape of transmissibility frequency curve has three regions depending on the degree of damping in the system: non-amplified region, amplified region, and isolation region. Resonance exists where transmissibility is maximized, and there is at least one resonant frequency for cushioning material. In particular, the composite materials such as a *MLCS* has more complicated transmissibility curve than uniform materials because of its internal non-uniformity (Guo et al., 2010; Guo et al., 2011). Generally, two to four primary peak frequencies exist in the transmissibility curve on shipping container, and the biggest one, whose transmissibility was five to ten times larger than others, was considered as the first principle mode (Figure 4). In this study, we focused on the analysis in the first principle mode.

This first principle mode of *MLCS* was again verified with the sinusoidal sweep vibration test (Figure 5); no significant difference was shown between both vibration tests. The transmissibility was significantly attenuated after the frequency passed the first principle mode.

Table 3 and Figure 6 show the resonant frequency and transmissibility of *MLCS* for each static stress at the different combination of paperboards and flute type. This

Table 2. *PSD* profile of the ASTM D4728

Mode of transport	Break point	Frequency (Hz)	*PSD* (G^2/Hz) by assurance level		
			I	II	III
Truck	1	1	0.0001	0.00005	0.000025
	2	4	0.02	0.01	0.005
	3	16	0.02	0.01	0.005
	4	40	0.002	0.001	0.0005
	5	80	0.002	0.001	0.0005
	6	200	0.00002	0.00001	0.000005
		Overall, G_{rms}	0.73	0.52	0.37

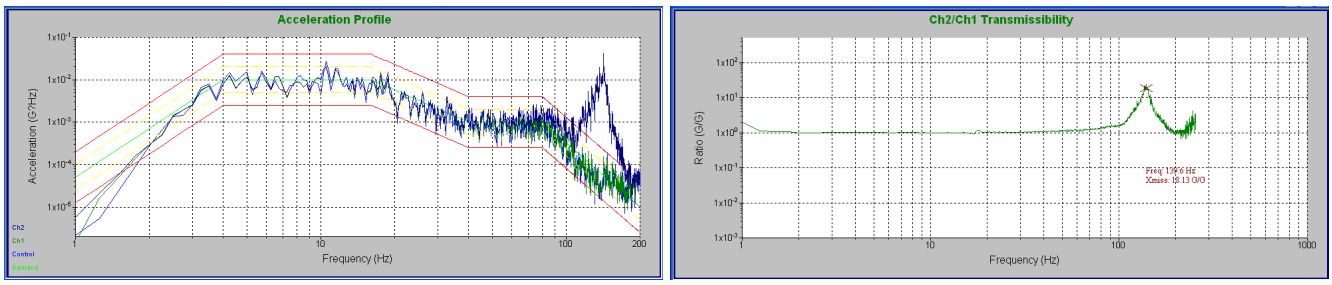

(a) vibration response (*PSD*) (b) vibration transmissibility

Figure 4. Example for vibration response and vibration transmissibility curves of *MLCS* by random vibration test (*K180*, *B/F*, thickness_30 mm, static stress_4.0 kPa).

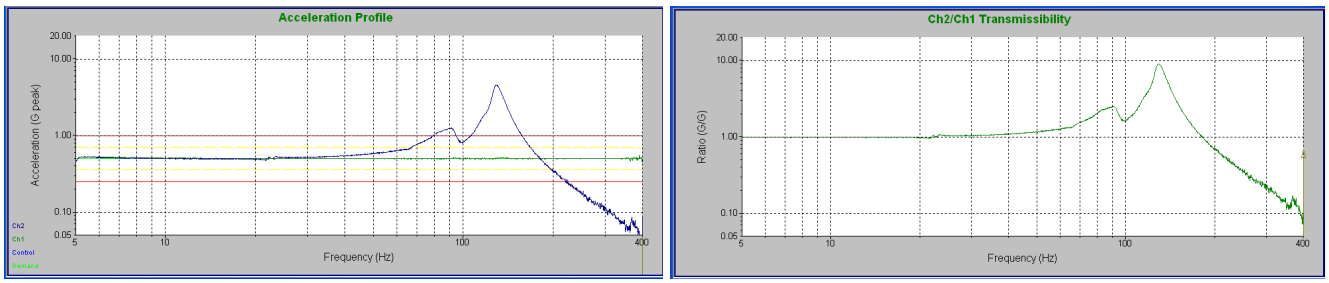

(a) vibration response (G's) (b) vibration transmissibility

Figure 5. Example for vibration response and vibration transmissibility curves of *MLCS* by sinusoidal sweep vibration test (*S120*, *B/F*, thickness_30 mm, static stress_4.0 kPa).

Table 3. Maximum vibration transmissibility (T_r), resonant frequency (f_r) and damping ratio (ζ) for each combination of flute type, static stress (s) and paperboards

Classifications		Thickness (mm)	Static stress level													
			1.5 kPa			4.0 kPa			6.5 kPa			9.0 kPa			11.5 kPa		
			f_r	T_r	ζ	f_r	T_r	ζ	f_r	T_r	ζ	f_r	T_r	ζ	f_r	T_r	ζ
S120	*A/F*	10	no	no	no	156	6.9	0.073	112	6.7	0.075	97	6.9	0.073	86	6.8	0.074
		30	175	10.0	0.050	104	6.7	0.075	70	6.8	0.074	55	5.5	0.092	45	4.1	0.126
		50	101	6.7	0.075	60	12.3	0.041	36	8.6	0.058	28	9.7	0.052	24	11.2	0.045
	B/F	10	no	no	no	186	10.7	0.047	142	12.8	0.039	127	9.8	0.051	116	11.5	0.044
		30	198	10.1	0.050	127	9.9	0.051	93	11.5	0.044	78	10.2	0.049	68	10.9	0.046
		50	116	11.0	0.046	75	13.4	0.037	51	10.8	0.046	41	12.1	0.041	40	11.7	0.043
K180	*A/F*	10	no	no	no	185	11.4	0.044	142	7.3	0.069	123	9.9	0.051	110	10.3	0.049
		30	191	12.7	0.040	115	10.2	0.049	82	11.1	0.045	62	8.7	0.058	55	9.4	0.053
		50	125	11.7	0.043	78	8.9	0.056	53	10.9	0.046	40	10.7	0.047	32	10.0	0.050
	B/F	10	no	no	no	no	no	no	172	13.4	0.037	153	15.7	0.032	140	14.2	0.035
		30	no	no	no	no	no	no	104	16.2	0.031	84	12.9	0.039	77	13.7	0.037
		50	140	13.1	0.038	93	14.8	0.034	68	11.2	0.045	55	14.7	0.034	47	14.6	0.034

'no' means impossibility of measurement and analysis in the study.

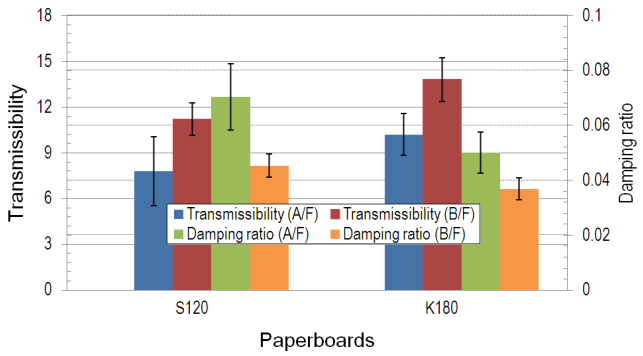

Figure 6. Vibration transmissibility (T_r) and damping ratio (ζ) for each combination of flute type and paperboards.

behavior could be well explained with the natural frequency model of cushioning material and block, showing that the *MLCS* has somewhat elastic characteristics.

The resonant frequency and transmissibility at *K180* were higher than the values at *S120*, and *B*-flute showed higher these values than *A*-flute as well. That is due to the material stiffness; under the same condition, each *K180* and *B*-flute was more stiff than *S120* and *A*-flute. As the material thickness increased, the resonant frequency decreased, whereas the vibration transmissibility didn't show a clear tendency.

A *MLCS* has shown an excellent performance in vibration isolation for high frequency range (Guo et al., 2010). We used the nonlinear least-squares (*NLLS*) Marquardt-Levenberg algorithm in DataFit software (Ver 9.0, Oakdale Engineering, Oakdale, PA, USA) to fit the resonant frequencies (f_r) with thickness (t) and static stress (s). Table 4 and Figure 7 show the model and estimated results of resonant frequency at different combination of paperboards

Table 4. Modelling results for resonance frequency (f_r) as a function of thickness (t) of cushion material and static stress (s)

Classifications		$f_r = a+bt+\frac{c}{s}+dt^2+\frac{e}{s^2}+f\left(\frac{t}{s}\right)$						r^2
		a	*b*	*c*	*d*	*e*	*f*	
S120	*A/F*	63.2346	-2.3270	566.5438	0.0192	-257.0382	-4.7808	0.9989
	B/F	96.3469	-2.6203	566.2615	0.0177	-256.9527	-4.7679	0.9989
K180	*A/F*	102.5139	-4.3576	610.7800	0.0470	-298.6139	-4.6211	0.9992
	B/F	136.8889	-4.8076	610.7800	0.0482	-298.6139	-4.6211	0.9993

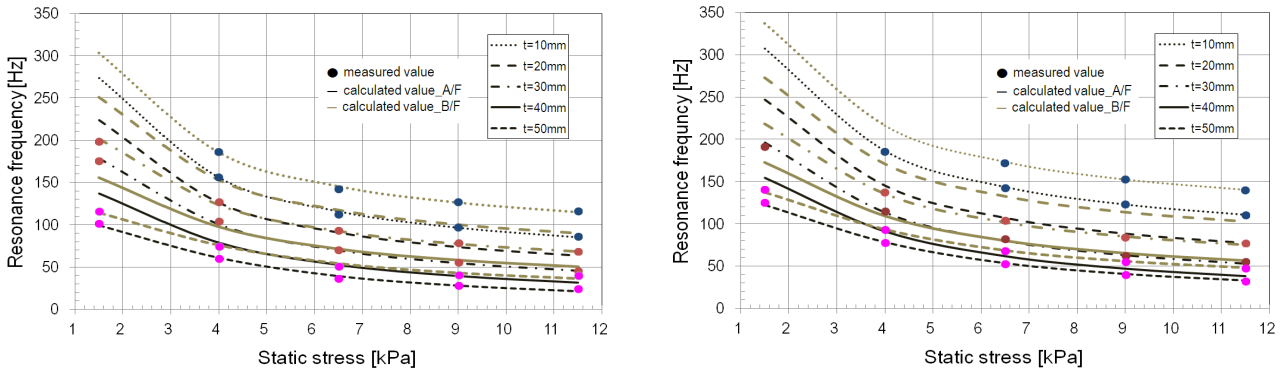

(a) paperboard_*S120* (b) paperboard_*K180*

Figure 7. Resonant frequency (f_r) for each combination of flute type and paperboards.

and flute type. The calculated resonant frequencies from the developed model were in good agreement with the measured values ($r^2 > 0.99$).

Estimation of the damping ratios of *MLCS*

The damping ratio of a cushioning material is defined by the ratio of the actual damping coefficient to the critical damping coefficient, and it can significantly affect the vibration transmissibility (Piersol and Paez, 2010). In this study, the damping ratios of *MLCS* were estimated using the linear vibration model developed with the relationship between the resonant frequency and vibration transmissibility of corrugated paperboards (Park et al., 2011). In order to induce this model, the cushioning material and block system were approximated to a one-degree of freedom vibration system as shown in Figure 8.

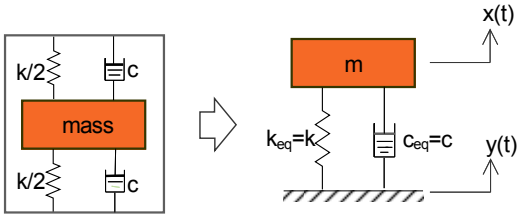

Figure 8. Linear vibration model for single-degree-of-freedom system.

A vibration equation was derived from the Newton's law of motion for a sinusoidal displacement with excitation input, $y(t)=B\sin(\omega t)$.

$$\left[\sum F = m\ddot{x}\right] \quad m\ddot{x}(t) = -c(\dot{x}-\dot{y}) - k(x-y) \tag{1}$$

where m is a mass of block, k is a stiffness coefficient for cushioning material, and c is a viscous damping coefficient of cushioning material.

A steady-state response for differential equation (1) is expressed by equation (2).

$$x = X\sin(\omega t - \phi) \tag{2}$$

$$X = B\left\{\frac{1+(2\zeta\lambda)^2}{(1-\lambda^2)^2+(2\zeta\lambda)^2}\right\}^{1/2},\ \phi = \tan^{-1}\left\{\frac{2\zeta\lambda^3}{1+(4\zeta^2-1)\lambda^2}\right\} \tag{3}$$

where ω is an excitation angular frequency of system, ω_n is a natural frequency of the system ($=\sqrt{k/m}$), λ is the frequency ratio ($=\omega/\omega_n$), and ζ is the damping ratio ($=c/2m\omega_n$).

Displacement transmissibility (T_r) can be defined with the ratio of response amplitude (X) to input displacement amplitude (B) in Equation (3). It is dimensionless value and can be applied to the transmissibility of force and accelerations as well. In addition, it can be expressed as a function of frequency and damping ratio [Equation (4)].

$$T_r = \frac{X}{B} = \left\{ \frac{1+(2\zeta\lambda)^2}{(1-\lambda^2)^2+(2\zeta\lambda)^2} \right\}^{1/2} \quad (4)$$

When the damping ratio is very small, since resonance normally occurs around $\lambda \fallingdotseq 1$, the damping ratio can be calculated using Equation (5) and was listed in Table 3.

$$\zeta = \frac{1}{2}\left(\frac{1}{T_r^2 - 1} \right)^{1/2} \quad (5)$$

The damping ratios in *S120* and *K180* were 0.07 and 0.04 for *A*-flute, and 0.05 and 0.03 for *B*-flute, respectively. It turns out that the damping ratios of *A*-flute were higher than the value of *B*-flute. Unlike vibration transmissibility, the damping ratio decreased as the material's stiffness increased.

Application of vibration amplification/attenuation plot

Properties of cushioning material, which are required for protecting products from shock and vibration, are clearly different. Generally, small damping is necessary for the vibration isolation of cushioning material; however, under-damping causes to diminish the resilience of cushioning material, resulting in increasing mechanical impact on the material. Therefore, both shock and vibration should be methodically considered in cushioning packaging design.

In cushioning packaging design, first, the cushion curves are selected with shock fragility and design drop height of the product, and thickness of material and an allowable static stress is determined using the cushion curve. A minimum static stress is determined with vibration fragility using the vibration amplification/attenuation plot of the same thickness of material as selected cushion curve. Third, the comparison between the allowable static stress and the minimum static stress is carried out to confirm the resonant response of the cushioning material.

Here is a case study of the application of vibration amplification/attenuation plot to the cushioning package

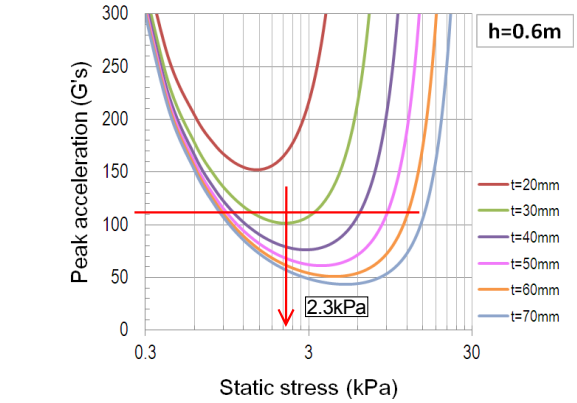

(a) Cushion curve_averaged 2nd~5th drop

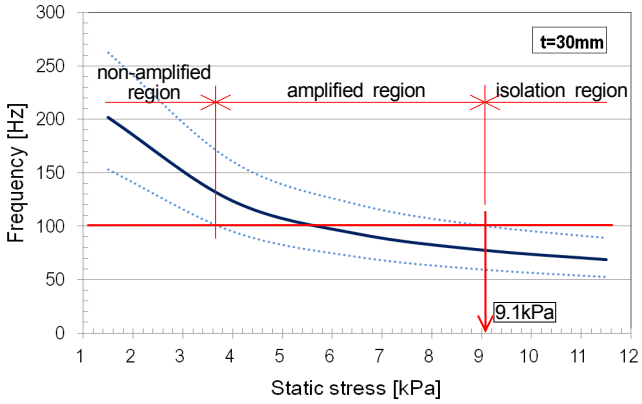

(b) Vibration amplification/attenuation plot

Figure 9. Cushion curves and vibration amplification/attenuation plot for *MLCS* (paperboard_*S120*, flute type_*B/F*).

design. The shock fragility was 110 G, the vibration fragility was 100 Hz, and the design drop height of product was 60 cm. Figure 9(a) shows the cushion curves at the design drop height of 60 cm in different sample thickness. At the shock fragility of 110 G, the sample thickness, 30 mm, and the allowable static stress, 2.3 kPa, were determined.

The vibration amplification/attenuation plot at the sample thickness of 30 mm is shown in Figure 9(b). In general, the amplification and attenuation boundaries are different largely on the material's stiffness, and the amplification zone becomes wider as the resonant frequency increases (Godshall, 1971). In this study, the amplification and attenuation boundaries were determined to ±30% range of resonance (Park et al. 2011). When the vibration fragility of product (100 Hz) meet the attenuation zone in Figure 9(b), the minimum static stress is 9.1 kPa.

The allowable static stress, 2.3 kPa, is located in the non-amplified region [Figure 9(b)]. If the allowable static stress was located in the amplified region and its transmissibility was higher than 5 (MIL-HDBK-304C),

cushioning packaging design should be performed again.

Conclusions

A paper-based packaging material is rapidly expanded to keep pace with the emerging issue of an environmental conservation. In particular, a multi-layered corrugated structure can be manufactured using standardized production facilities without using a special mold. Besides the versatility, a short packaging development period makes it being more attractive as a cushioning packaging material option.

Both cushion curve and vibration amplification/attenuation plot are indispensable to design or select the optimal multi-layered corrugated structure as a cushioning packaging material.

Therefore, we analyzed resonant frequency, transmissibility and damping ratio of multi-layered corrugated structure using random vibration test in different paperboards and flute types. The main results are summarized as follows.

(1) The resonant frequency was decreased as the static stress increased, which means that the multi-layered corrugated structure had an elastic characteristic. In addition, the resonant frequency at the multi-layered corrugated structure of *K180* was higher than *S120*, and *B*-flute also had the higher value than *A*-flute.
(2) The transmissibility of multi-layered corrugated structure was independent on the static stress and sample thickness. However, like resonant frequency, the transmissibility at *K180* and *B*-flute were each higher than the value at *S120* and *A*-flute.
(3) Unlike the transmissibility, the damping ratio at *K180* and *B*-flute were each lower than the value at *S120* and *A*-flute.
(4) A compromise problem between shock and vibration for optimal cushioning packaging design as well as the practical application of the developed model were discussed and demonstrated with a case study.

Conflict of Interest

The authors have no conflicting financial or other interests.

Acknowledgements

This work was supported for two years by Pusan National University Research Grant.

References

ASTM. 2012. ASTM Standards D4728-06: Standard test method for random vibration testing of shipping containers. *Annual Book of ASTM Standards*, West Conshohocken, PA: ASTM International.

Godshall, W. D. 1971. Frequency response, damping, and transmissibility characteristics of top-loaded corrugated container. FPL:1-12.

Guo, Y. F. and J. H. Zhang. 2004. Shock absorbing characteristics and vibration transmissibility of Honeycomb Paperboard. Shock and Vibration 11:521-531.

Guo, Y. F., Y. G. Fu, and W. Zhang. 2008. Creep properties and recoverability of double-wall corrugated paperboard. Experimental Mechanics 48(3):327-333.

Guo, Y., Xu, W., Fu, Y. and Zhang, W. 2010. Comparison Studies on Dynamic Packaging Properties of Corrugated Paperboard Pads. Engineering, 2(5):378.

Guo, Y., Xu, W., Fu, Y. and Wang, H. 2011. Dynamic shock cushioning characteristics and vibration transmissibility of X-PLY corrugated paperboard. Shock and Vibration, 18(4):525-535.

MIL-HDBK-304C : Package cushioning design.

Park, J. M. et al. 2011. Characteristics of vibration transmissibility for corrugated paperboard. Journal of the faculty of agriculture, Kyushu Univ. 56(2):327-333.

Piersol, A. G. and T. L. Paez. 2010. Harris' shock vibration handbook (6th Edition). McGraw-Hill.

Rouillard, V. and M. A. Sek. 2007. Behaviour of multi-layered corrugated paperboard cushioning systems under impact loads. Strain 43:345-347.

Sek, M. and J. Kirkpatrick. 1997. Prediction of the cushioning properties of corrugated fiberboard from static and quasi-dynamic compression data. Packaging Technology & Science 10(2):87-94.

Wang, D. M. and Z. W. Wang. 2008. Experimental investigation into the cushioning properties of honeycomb paperboard. Packaging Technology and Science 21(6): 309-316.